Available online at www.sciencedirect.com
SCIENCE DIRECT®
Polymer 44 (2003) 6647–6656
polymer
www.elsevier.com/locate/polymer

Crystallization and orientation behaviors in isotactic polystyrene and poly(2,6-dimethylphenylene oxide) blends

Asok K. Dikshit, Akira Kaito*

National Institute of Advanced Industrial Science and Technology, Research Center of Macromolecular Technology, Tokyo Waterfront, 2-41-6 Aomi, Koutou-ku, Tokyo 135-0064, Japan

Received 27 May 2002; received in revised form 16 April 2003; accepted 5 August 2003

Abstract

The crystallization and orientation behavior in the miscible iPS/PPO blends were studied aiming at producing oriented materials consisting of iPS crystals and amorphous PPO chains. Oriented films of iPS/PPO blends were prepared by drawing the melt-quenched blend films. The films were heat-treated under constraint at the drawing temperature so as to crystallize the molecular chains of iPS in the oriented state. The crystallinity and the crystal orientation in the drawn annealed films were studied by the wide-angle X-ray diffraction (WAXD), and the orientation behaviors of molecular chains were analyzed by polarized FTIR spectroscopy. WAXD diagrams show the presence of the highly oriented crystalline structure of iPS in the drawn annealed films of pure iPS and iPS/PPO = 7/3 blend. The polarized FTIR spectra of drawn annealed films suggest that the molecular orientation of the amorphous chains of PPO and iPS is markedly relaxed by the heat treatment, although the orientation of iPS with 3_1 helical structure was retained during the oriented crystallization. It was concluded that the drawn annealed samples of the iPS/PPO = 7/3 blend consist of highly oriented iPS crystals and nearly isotropic amorphous materials. The mechanical properties of the oriented iPS/PPO blends were measured not only in the stretching direction but also perpendicular to the stretching direction. It was shown that the ultimate strength in the perpendicular direction is 4–5 times higher in the drawn annealed film of iPS/PPO = 7/3 blend than in the drawn annealed iPS. The improvement in the vertical strength in the blend is discussed in relation to the structural characteristics of the iPS/PPO blend.

Keywords: Isotactic polystyrene and poly(2,6-dimethylphenylene oxide) blends; Crystallization; Molecular orientation

1. Introduction

Isotactic polystyrene (iPS) is one of the commercially potential polymers in our global market because of its excellent mechanical and thermal properties and dimensional stability, etc. It was reported that iPS forms compatible blends with poly(2,6-dimethylphenylene oxide) (PPO) [1–3]. Although iPS crystallizes even in the compatible blends, the miscibility of iPS and PPO in the amorphous phase was supported by the observation of single glass transition temperature (Tg) and by the large depression in the melting temperature of iPS in the blend [3]. The morphological superstructure of the crystallized iPS/PPO blends was analyzed by small-angle X-ray scattering (SAXS) [1] and wide-angle X-ray diffraction (WAXD) [2]. The formation of compatible blends of iPS with PPO further suggests the possibility of controlling the physical properties of the polymers.

On the other hand, the orientation of polymer chains is one of the important factors in controlling the mechanical properties of polymers. In spite of extensive studies on molecular orientation of polymers, a few studies have been reported on the orientation of polymer blends. The molecular orientation of polymer blends is an attractive subject, because the two components possibly orient in a different way, which leads to the formation of new superstructure of blend systems. Monnerie et al. studied the orientation behavior of the aPS/PPO blends by polarized Fourier transform infrared (FTIR) spectroscopy [4–6]. The orientation of PPO does not depend upon PPO content while the orientation function of PS increases with increase in PPO content up to 25%. Abtal and Prud'homme studied the orientation behavior of atactic polystyrene/ poly(vinyl

* Corresponding author. Tel.: +81-3-3599-8307; fax: +81-3-3599-8166.
E-mail address: a-kaito@aist.go.jp (A. Kaito).

0032-3861/$ - see front matter © 2003 Elsevier Ltd. All rights reserved.
doi:10.1016/j.polymer.2003.08.017

methyl ether) blends and reported that the orientation function is much higher in the blends with 50% PVME composition than in the pure aPS [7].

More recently Prud'home reported the crystallization of poly(ε-caprolactone) (PCL) in the stretched miscible blends with poly (vinyl chloride) (PVC) [8,9]. It was found that, under most conditions, the crystallization under strain leads to a crystalline orientation perpendicular to the strain direction, whereas a parallel crystalline orientation is observed under conditions where the crystallization is rapid and the draw ratio is high.

In the present work, we report the crystallization and orientation behavior in the miscible iPS/PPO blends aiming at producing oriented materials consisting of iPS crystals and amorphous chains of PPO. The crystallinity and the crystal orientation were studied by WAXD, and the orientation behaviors of iPS and PPO molecular chains were obtained by polarized FTIR spectroscopy. In addition, the mechanical properties of the oriented iPS/PPO blends were measured not only in the stretching direction but also perpendicular to the stretching direction.

2. Experimental

2.1. Materials and sample preparation

The samples used in this work are powdered isotactic polystyrene (90% isotacticity) with M_w of 400,000 and poly(2,6-dimethylphenylene oxide) with M_w of 50,000 and a polydispersity index of 1.9 (Scientific Polymer Products Company, Limited). The iPS/PPO blends with the molar ratio of 7/3 and 5/5 were prepared by casting the chlorobenzene solution with a concentration of 0.4–0.6 wt%. The films were dried at 80 °C under vacuum for 2 days in order to remove the solvent. The blend films were hot pressed at 230 °C under nitrogen stream and subsequently quenched into ice water to obtain amorphous blend film. The amorphous films of pure iPS were prepared by quenching the molten film in the same way as in the blend films.

The samples were stretched into a draw ratio, λ, of 2–6 using a hand-operated stretching instrument and a hot oven with a temperature accuracy of ±1.5 °C. The drawing temperature was set at 100, 135, and 160 °C for pure iPS, iPS/PPO = 7/3 blend, and iPS/PPO = 5/5 blend, respectively. The sample can be drawn to the higher draw ratio at higher drawing temperature, but the orientation is markedly relaxed at higher drawing temperature. On the other hand, it is difficult to stretch the polymer film at lower temperature than the drawn temperature studied in this work.

The drawn samples were heat-treated with the dimension fixed at the stretching temperature for 24 h in a temperature-controlled vacuum oven. At higher annealing temperature, the crystallization time is shortened, but the relaxation of orientation becomes marked.

2.2. Characterization

Differential scanning calorimetry (DSC) was measured under nitrogen flow at a heating rate of 10 K/min with a Perkin Elmer DSC-7 differential scanning calorimeter calibrated with indium and zinc.

WAXD pattern was measured with the imaging plates (IP) using a monochromatized Cu Kα radiation of wavelength 0.1542 nm (40 kV, 200 mA) generated by Rotaflex RU-300 X-ray diffractometer (Rigaku Co. Ltd). The WAXD profiles were obtained from the IP as digitized data using an imaging plate reader, Rigaku RAXIS DS.

The orientation function is defined as

$$f = (3\langle\cos^2\phi\rangle - 1)/2 \quad (1)$$

where ϕ is the angle between the corresponding crystal axis and the stretching direction. The crystal orientation function of the [110] axis was calculated from the azimuthal intensity distribution of the 220 reflection at $2\theta = 16.2°$ (θ: Bragg angle).

The polarized FTIR spectra were recorded at a resolution of 4 cm^{-1} with a Bio-rad FTS 60A-686 FTIR spectrophotometer equipped with a wire-grid polarizer.

Mechanical properties were characterized not only in the stretching direction, but also in the direction perpendicular to it. Rectangle-shaped specimens 2 mm wide and 20 mm long were cut from the samples, and were used for the tensile test. Tensile tests were carried out at 20 °C and 50% relative humidity, using a Tensilon UMT-300 (Orientec Co. Ltd) at a strain rate of 0.2/min. The dynamic mechanical properties were measured from −150 to 180 °C at a heating rate of 3 °C/min under nitrogen stream using a dynamic viscoelastometer, Rheovibron DDV-01FP. The Lissajous figures were monitored during the measurements. The dynamic mechanical properties at the lower temperatures were obtained by cooling the system with liquid nitrogen. The rectangle-shaped specimen with a dimension of 2×20 mm^2 were cut from the specimen, and the measurements were carried out with application of dynamic and static tensile forces. A dynamic strain with amplitude of 0.03% of the gauge length and a frequency of 5 Hz was applied to the sample as well as the static stress.

3. Results and discussion

3.1. Thermal properties

Fig. 1 shows the DSC thermograms of pure iPS, pure PPO, and the iPS/PPO blends with compositions of iPS/PPO = 7/3, 5/5, 3/7. All of them are obtained by quenching the melts to ice water at 0°. The glass transition temperature, Tg, of pure iPS and PPO are 96 and 210 °C, respectively. The crystallization and melting peaks are observed at 164 and 222 °C, respectively, in the DSC curve of pure iPS. The

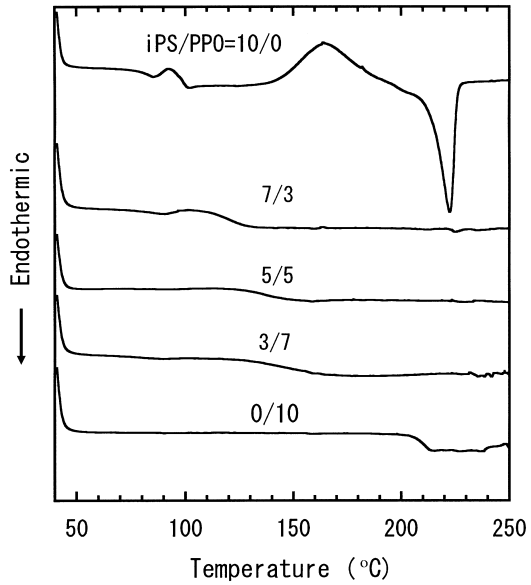

Fig. 1. DSC thermograms of melt-quenched samples of iPS, PPO, and iPS/PPO blends with compositions of iPS/PPO = 7/3, 5/5, 3/7.

enthalpy change ΔH_c during crystallization is in good agreement with the enthalpy change, ΔH_m during melting and henceforth the melt-quenched iPS is amorphous in nature as well as the other quenched samples. A single glass transition is observed for each blend sample, suggesting that the iPS/PPO system is miscible in the amorphous phase as reported in Refs. [1–3]. Tg shifts toward the higher temperature with increase in PPO content.

3.2. WAXD studies

Fig. 2 shows the WAXD diagrams of drawn samples of pure iPS, iPS/PPO = 7/3 and 5/5 blends before and after annealing. The WAXD diagram shows the presence of highly oriented crystalline morphology of iPS crystals for the as-drawn sample (before annealing) with a draw ratio, $\lambda = 5$ (Fig. 2a). The 110, 300, and 220 reflections are observed at $2\theta = 8.2$, 13.9, and 16.2°, respectively on the equator, and the 211 reflection appears at $2\theta = 18.2°$ on the diagonal position. The intensities of the crystal reflections are markedly reduced in the as-drawn sample of iPS/PPO = 7/3 blend (Fig. 2b), and only the amorphous hallo is observed in the WAXD diagram of the iPS/PPO = 5/5 blend before annealing (Fig. 2c). These results show that the crystallization of iPS is induced by the orientation of molecular chains and that blending the PPO amorphous diluent restricts the oriented crystallization. The crystal reflections are observed more clearly in the annealed samples of pure iPS and iPS/PPO = 7/3 blend than in their as-drawn samples (Fig. 2d and e). The crystallization occurs in the drawn sample of iPS/PPO = 5/5 blend with draw ratios 5 and 6 by annealing at the drawing temperature for 24 h (Fig. 2f). Thus the oriented crystallization is more

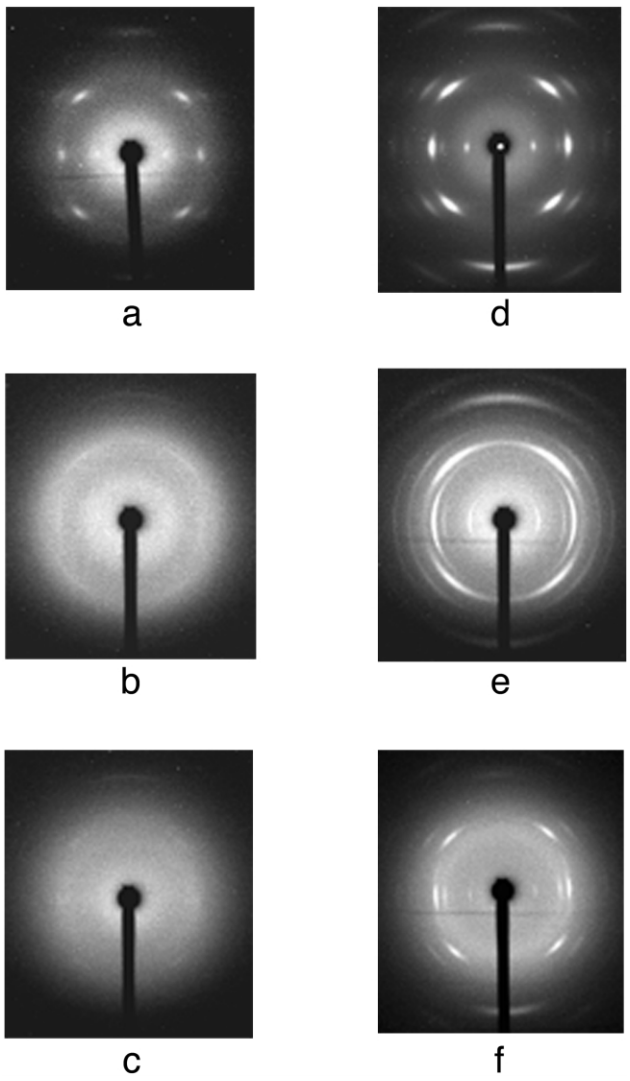

Fig. 2. WAXD diagrams of drawn samples: (a) pure iPS, as-drawn; (b) iPS/PPO = 7/3, as-drawn; (c) iPS/PPO = 5/5, as-drawn; (d) pure iPS, after annealing; (e) iPS/PPO = 7/3, after annealing; (f) iPS/PPO = 5/5, after annealing.

prominent in the annealed samples than in the as-drawn samples.

Fig. 3 shows the crystallinity of stretched samples at various draw ratios. The WAXD profiles of samples were resolved into crystalline and amorphous reflections, and the degree of crystallinity was obtained from the ratio of the intensity of the crystal and amorphous reflections. The strain-induced crystallization occurs by stretching the amorphous films of pure iPS and iPS/PPO = 7/3 blend into draw ratio higher than 3 and 4, respectively. The iPS/PPO = 5/5 blend does not crystallize even when it is stretched into the highest draw ratio. The degrees of crytallinity of drawn annealed samples of pure iPS and iPS/PPO = 7/3 lie in the range of 26–35%. The drawn annealed films of iPS/PPO = 5/5 blend are amorphous up to draw ratio 4, but it starts to increase at draw ratio 5.

Fig. 4 shows the crystal orientation function as a function

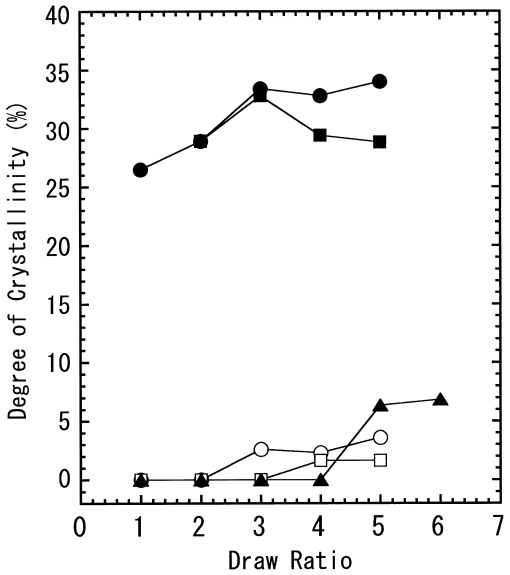

Fig. 3. The degree of crystallinity vs. draw ratio: (○) as-drawn films of pure iPS; (●) drawn annealed films of pure iPS; (□) as-drawn films of iPS/PPO = 7/3 blend; (■) drawn annealed films of iPS/PPO = 7/3 blend; (▲) drawn annealed films of iPS/PPO = 5/5 blend.

of draw ratio. The orientation function of the [110] axis, f_{110} was obtained from the azimuthal intensity distribution of the 220 reflection, and the orientation function of the crystal *c*-axis, f_c was obtained by use of the equation, $f_c = -2f_{110}$, which holds in the case of hexagonal crystal lattice. The orientation function of drawn annealed film of pure iPS increases with increasing draw ratio from 2 to 3, and becomes constant in the draw ratio range of 3–5. For the annealed films of iPS/PPO = 7/3 blend, the orientation function increases from draw ratio 2 to 5, and the increase of

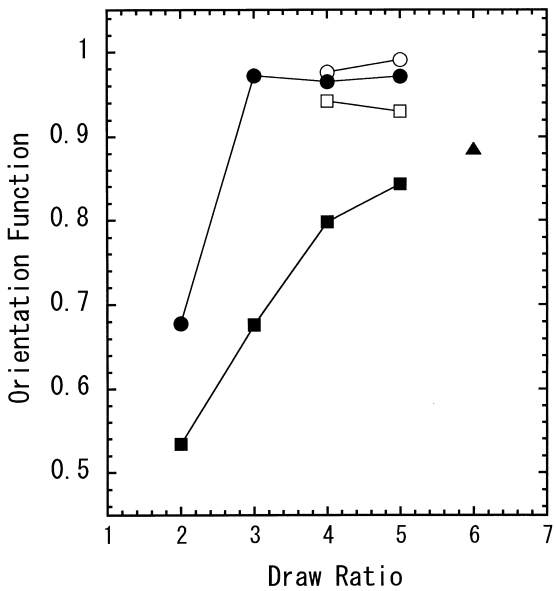

Fig. 4. Orientation function vs. draw ratio: (○) as-drawn films of pure iPS; (●) drawn annealed films of pure iPS; (□) as-drawn films of iPS/PPO = 7/3 blend; (■) drawn annealed films of iPS/PPO = 7/3 blend; (▲) drawn annealed films of iPS/PPO = 5/5 blend.

the orientation function becomes gradual at higher draw ratio. The orientation of the iPS crystals is partially relaxed by the heat-treatment for the iPS/PPO = 7/3 blend (Table 1).

3.3. FTIR studies

Fig. 5 shows the FTIR spectra of quenched films of iPS and PPO. The spectra were normalized by the film thickness. The absorption bands are strongly overlapping to each other in the wavenumber region of 1000–1400 cm^{-1}, whereas the absorption bands of the two components are separated from each other in the wavenumber region below 1000 cm^{-1}. PPO shows intense IR bands at 960, 858, and 836 cm^{-1}, and iPS gives rise to absorption at 908, 762, 700, and 558 cm^{-1}. Fig. 6 shows the polarized FTIR spectra of the drawn annealed film of pure iPS. A lot of new absorption bands are observed with large dichroism in the polarized FTIR spectra of the drawn annealed film of pure iPS with draw ratio 5. The appearance of the new band is attributable to the conformational change to the 3_1 helical structure, which occurs during oriented crystallization of iPS. The conformational change during crystallization has been extensively studied with in situ FTIR spectroscopy, and the ordered conformation was shown to appear prior to the beginning of crystallization [10–12].

The bands at 1364, 1312, 1297, 1194, 1084, 1050, 981, 920, 898, 783, and 758 cm^{-1} originate from the 3_1 helical structure of iPS consisting of *trans* (T)/*gauche* (G) conformation [13,14]. The intensities of the helix bands are much sensitive to the sequence length of the helix, and the critical sequence length that is needed to observe the helix band, depends upon the bands [13,14]. On the other hand, it was reported that the 1185 and 981 cm^{-1} bands markedly increase in absorption intensity upon crystallization, although they have very low absorption intensity in solution [13]. The critical length of the helical sequence is considered to be longer for the 1185 and 981 cm^{-1} bands than that for the other helix bands. Out of these helix bands, we used the 981 cm^{-1} band for the structural analysis of iPS, because this band is most sensitive to the crystallization and is well isolated from the other absorption bands. The 981 cm^{-1} band is assigned to the CH out-of-plane bending vibration of benzene ring of iPS [15].

In addition, the spectra of the crystallized sample are markedly different from that of the amorphous sample in the wavenumber region of 500–600 cm^{-1}. The sharp absorption at 566 cm^{-1} is intensified in the crystallized sample relative to the spectrum of the amorphous sample. The 566 cm^{-1} band was reported to originate from the benzene rings, which are aligned regularly to the chain axis [13,16]. Thus the ordered structure of benzene rings is developed by the conformational transition during crystallization.

Fig. 7a and b show the polarized FTIR spectra of iPS/PPO = 7/3 blend with draw ratio 5 before and after annealing, respectively. All absorption bands in the range

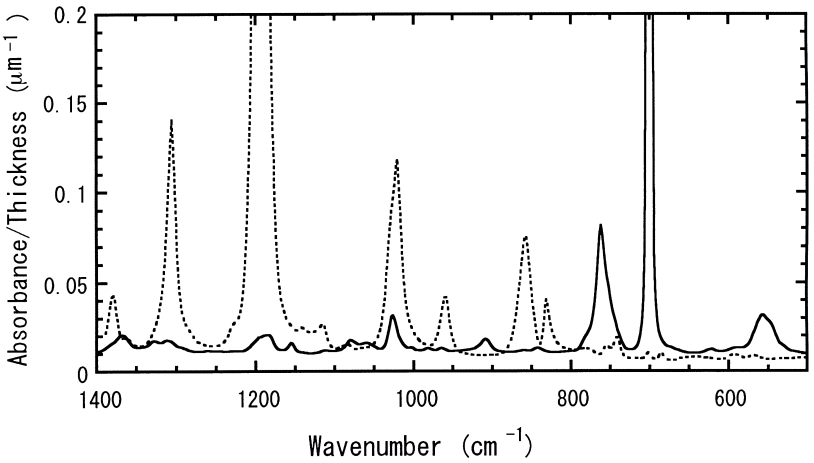

Fig. 5. FTIR spectra of amorphous films of iPS (——) and PPO (– – –): the spectra are normalized by the film thickness.

of 500–1000 cm^{-1} show dichroism in the spectra of as-drawn sample (Fig. 7a) showing that the molecular chains of both iPS and PPO are oriented before annealing. In the spectra of the annealed sample (Fig. 7b), however, the dichroism disappears for the absorption bands of PPO (960, 858, and 836 cm^{-1}), and the 3_1 helix bands of iPS (920, 898, 783, 758, and 700 cm^{-1}) are intensified with the large dichroism retained. The results show that the orientation of PPO chains is relaxed during the heat- treatment and that the highly oriented molecular chains of iPS with 3_1 helical structure are developed by the oriented crystallization.

Fig. 8 shows the orientation function of 3_1 helical sequence of iPS determined from the dichroic ratio of the 981 cm^{-1} band. The orientation functions were calculated by the equation

$$f = (D - 1)/(D + 2), \quad (2)$$

where D is the dichroic ratio obtained from the integrated area intensity of the absorption bands. The value of orientation function decreases with the increase in the degree of orientation of molecular chains, because of the perpendicular alignment of the transition moment against the chain axis. The results in Fig. 8 show that the degree of orientation of 3_1 helical sequence of iPS increases almost linearly with increasing draw ratio. The orientation function is not significantly affected by the composition and the heat-treatment at lower draw ratio.

Both WAXD and FTIR results show that the molecular orientation of iPS increases with draw ratio for both pure iPS and iPS/PPO blends (Figs. 4 and 8). There are some differences in the results of orientation obtained by WAXD and polarized FTIR. The orientation function obtained from WAXD represents the orientation of crystallite, whereas the polarized FTIR reveals the orientation function of molecular chains both in crystal and amorphous phases. The absorption intensity of 981 cm^{-1} band starts to increase at the lower draw ratio, at which the crystal reflection does not appear in the WAXD. The orientation function of 3_1 helical molecular chains increases almost linearly with draw ratio, whereas the increase in the crystal orientation function tends to saturate at the high draw ratio. These results suggest that there are significant contributions from the oriented 3_1 helical sequences in the amorphous region to the intensity of 981 cm^{-1} band in the polarized FTIR spectra.

Fig. 9 shows the orientation function of the amorphous chains of PPO, which was evaluated from the dichroic ratio

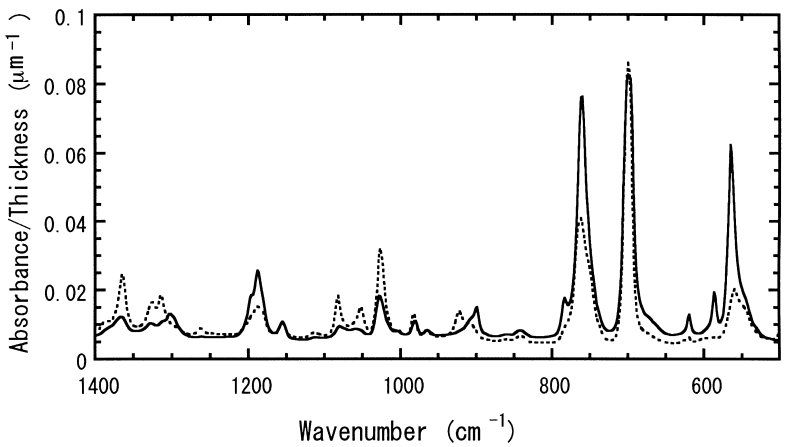

Fig. 6. Polarized FTIR spectra of the drawn annealed film of pure iPS: (——) parallel polarization; (– – –) perpendicular polarization.

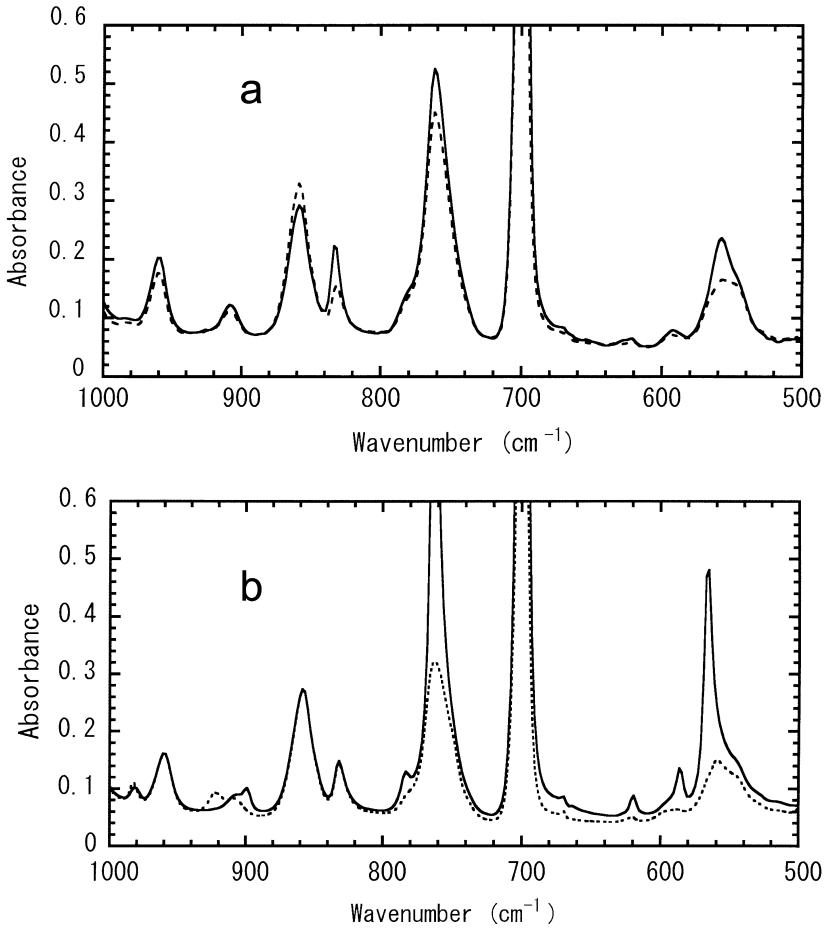

Fig. 7. Polalized FTIR spectra of iPS/PPO = 7/3 blend with draw ratio 5 (a) before annealing and (b) after annealing: (——) parallel polarization; (– – –) perpendicular polarization.

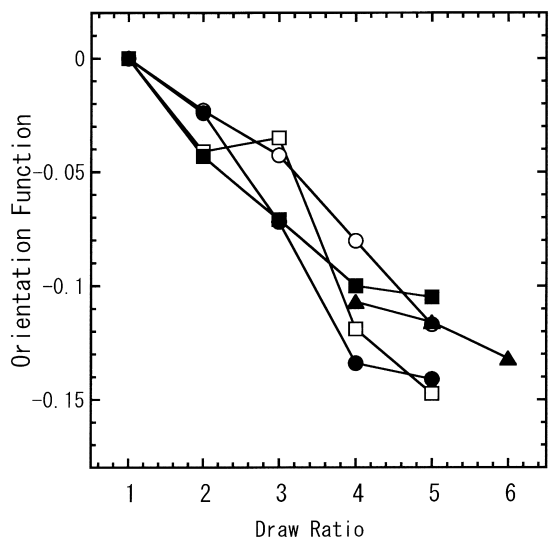

Fig. 8. The orientation function of 3_1 helical sequence of iPS determined from the dichroic ratio of the 981 cm^{-1} band: (○) as-drawn films of pure iPS; (●) drawn annealed films of pure iPS; (□) as-drawn films of iPS/PPO = 7/3 blend; (■) drawn annealed films of iPS/PPO = 7/3 blend; (▲) drawn annealed films of iPS/PPO = 5/5 blend.

of the 858 cm^{-1} band. The 858 cm^{-1} band is assigned to the out-of plane bending vibration of the 1,2,4,6-tetrasubstituted benzene ring of PPO [17]. The orientation function of the 858 cm^{-1} band decreases as the molecular chains align parallel to the draw direction, because the transition moment of the band is nearly perpendicular to the chain axis. The degree of orientation of molecular chains of PPO increases with increasing draw ratio in the as-drawn samples, while the molecular orientation of PPO is markedly relaxed in the annealed samples.

Prud'homme et al. reported that the crystallization of PCL in stretched miscible amorphous blends with PVC leads to the two types of orientation; either parallel or perpendicular to the drawing condition, depending upon the composition and draw ratio [8,9]. The parallel orientation was explained by an epitaxial growth of folded chain crystals from row nuclei as was discussed in the oriented crystallization of the cross-linked polymer. The perpendicular orientation is explained by the result of the folding of oriented chains. The perpendicular orientation is not produced in the case of iPS/PPO blends at any draw ratio and any composition studied, and the orientation of the amorphous component (PPO) is completely relaxed in the case of iPS/PPO blends. The mechanism of the

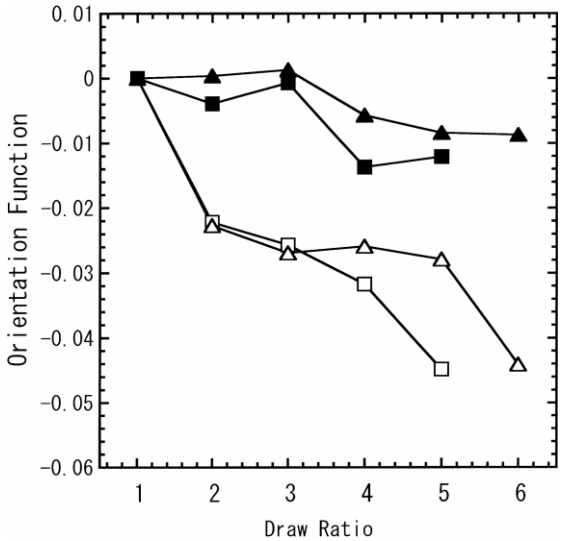

Fig. 9. The orientation function of the amorphous chains of PPO, determined from the dichroic ratio of the 858 cm^{-1} band: (□) as-drawn films of iPS/PPO = 7/3 blend; (■) drawn annealed films of iPS/PPO = 7/3 blend; (△) as-drawn films of iPS/PPO = 5/5 blend; (▲) drawn annealed films of iPS/PPO = 5/5 blend.

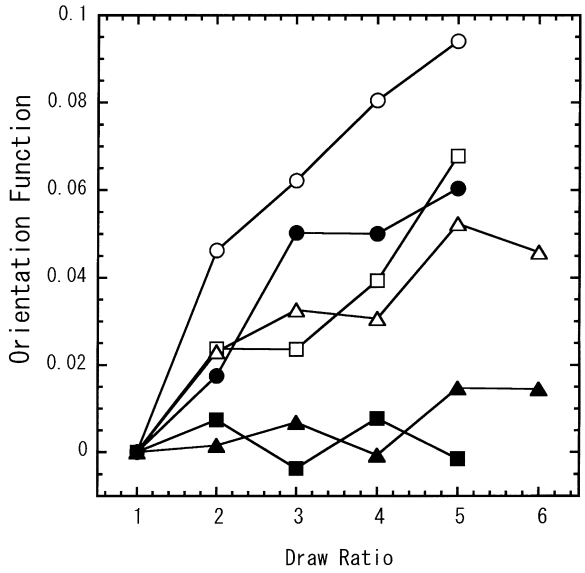

Fig. 10. The orientation function of the amorphous chains of iPS, determined from the dichroic ratio of the 907 cm^{-1} band: (○) as-drawn films of pure iPS; (●) drawn annealed films of pure iPS; (□) as-drawn films of iPS/PPO = 7/3 blend; (■) drawn annealed films of iPS/PPO = 7/3 blend; (△) as-drawn films of iPS/PPO = 5/5 blend; (▲) drawn annealed films of iPS/PPO = 5/5 blend.

crystallization of iPS/PPO blend is different from that in the PCL/PVC blend.

Fig. 10 shows the orientation function determined from the 908 cm^{-1} band. The 908 cm^{-1} band is considered to originate from the amorphous chains of iPS with the disordered conformation, because this band is strongly observed in the atactic PS films [15]. In the spectra of crystallized sample, the 898 and 920 cm^{-1} bands strongly overlap with the 908 cm^{-1} band. The absorption intensity of the 908 cm^{-1} band is obtained, after the contributions of 898 and 920 cm^{-1} bands are subtracted by the curve analysis. The orientation function in pure iPS increases with draw ratio, and the orientation function is lowered in the drawn annealed iPS relative to that in the as-drawn iPS with the same draw ratio. The orientation function for as-drawn samples of iPS/PPO = 7/3 and 5/5 blends are lower than the as-drawn pure iPS with the same draw ratio. The blending of PPO with iPS lowers the degree of orientation of amorphous iPS chains with disordered conformation. In addition, the orientation is markedly relaxed for the drawn annealed samples of iPS/PPO = 7/3 and 5/5 blends, as is observed in the orientation function of PPO chains.

Thus the oriented crystallization of iPS occurs in the drawn annealed samples of iPS/PPO = 7/3 blend but the orientation of amorphous chains of iPS and PPO are relaxed by the heat treatment.

3.4. Mechanical properties

Figs. 11 and 12 show the dynamic viscoelasticity of drawn annealed samples of pure iPS and iPS/PPO = 7/3 blend, respectively, with draw ratio 5. The dynamic viscoelasticity was measured both in the stretching direction (Figs. 11a and 12a) and in the perpendicular direction (Figs. 11b and 12b). Dynamic storage modulus of pure iPS with draw ratio 5 is nearly twice as high as in the stretching direction as that in the perpendicular direction in the temperature range of − 150 to 90 °C, and the similar result is obtained for the iPS/PPO = 7/3 blend. The dynamic viscoelasticity could not be measured in the perpendicular direction in the higher temperature range, because the samples are softened above glass transition and are elongated by the applied stress. The change of dynamic storage modulus is very gradual and the loss modulus does not show any peak below 80 °C for pure iPS (below 100 °C for iPS/PPO = 7/3 blend) suggesting that there is not any significant relaxation process below glass transition. The dynamic loss modulus of pure iPS shows a peak at 95–105 °C, which is close to the glass transition temperature measured by the DSC measurement. Analogously the dynamic loss modulus of iPS/PPO = 7/3 blend shows a peak at the location of the glass transition temperature.

Fig. 13 shows the stress–strain curves of the drawn annealed film of pure iPS with draw ratio 5 tested in the parallel and perpendicular directions. The oriented iPS film exhibits a maximum at a strain of 0.04 in the stress–strain curve in the parallel direction and the film is further deformed to a strain of 0.1. The ultimate strength of the oriented film in the parallel direction is nearly twice as high as the strength of isotropic iPS film (46 MPa), whereas the strength is as low as 13 MPa in the perpendicular direction. The drawn annealed films of pure iPS are very fragile in the perpendicular direction and are easily fractured at low stress and low strain.

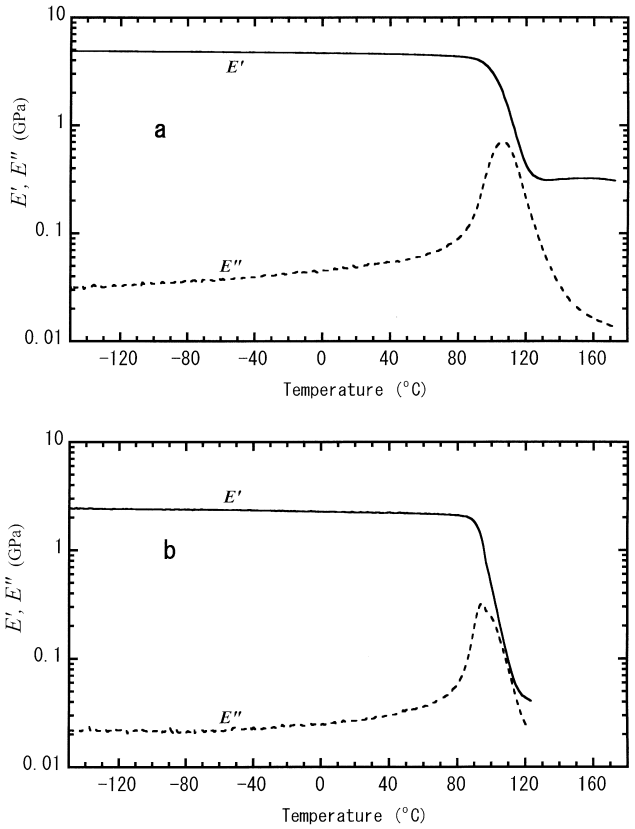

Fig. 11. Dynamic storage modulus, E' (——) and dynamic loss modulus, E'' (– – – –) of drawn annealed samples of pure iPS with draw ratio 5: (a) parallel direction; (b) perpendicular direction.

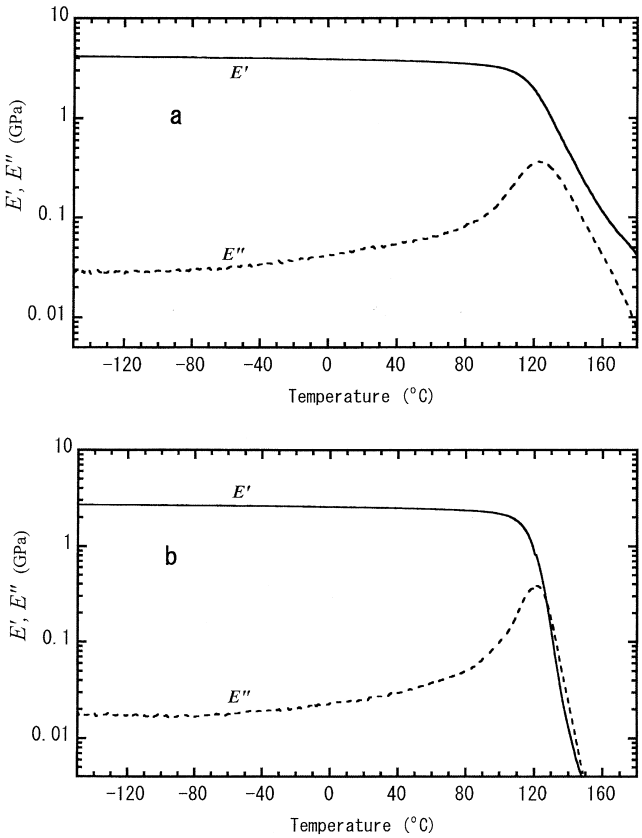

Fig. 12. Dynamic storage modulus, E' (——) and dynamic loss modulus, E'' (– – – –) of drawn annealed samples of iPS/PPO = 7/3 blend, with draw ratio 5: (a) parallel direction; (b) perpendicular direction.

Fig. 14 shows the stress–strain curves of the drawn annealed film of iPS/PPO = 7/3 blend with draw ratio 5. The ultimate strength in the parallel direction is a little lower in the oriented blend film than in the oriented iPS, whereas the strength in the perpendicular direction is much improved in the blend relative to the strength of the pure iPS with the same draw ratio. The ultimate strength in the perpendicular direction is much improved in the oriented blend films and the value is close to the strength of the isotropic iPS.

The mechanical properties of iPS and iPS/PPO blend films are summarized in Tables 1 and 2. The dynamic storage moduli of the as-drawn films of iPS/PPO blends with low degree of crystallinity are similar to the modulus of the isotropic sample both in the parallel and perpendicular directions, suggesting that the orientation of amorphous chains does not cause a large anisotropy of the modulus. The dynamic storage modulus in the parallel direction increases with increasing draw ratio and that in the perpendicular direction decreases with draw ratio in the drawn annealed samples of iPS/PPO blends and pure iPS. The oriented crystallization of iPS due to annealing induces an anisotropy in the dynamic storage modulus of the drawn film of iPS/PPO blends.

The ultimate strength increases with increasing draw ratio in the parallel direction, but decreases in the perpendicular direction. The decrease of the strength in the perpendicular direction is more marked in the pure iPS than in the iPS/PPO blends. The ultimate strength in the perpendicular direction is 4–5 times higher in the drawn annealed film of iPS/PPO = 7/3 blend than in the drawn annealed pure iPS. The iPS/PPO blend system shows a synergetic effect on the ultimate strength. The ultimate

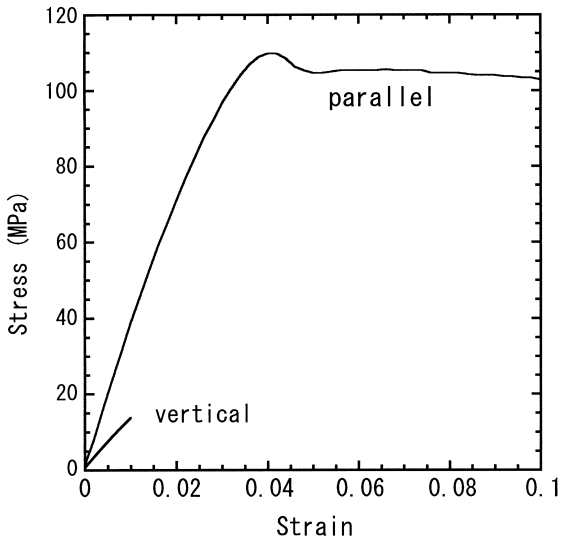

Fig. 13. Stress–strain curves of the drawn annealed film of pure iPS with draw ratio 5 tested in the parallel and perpendicular direction.

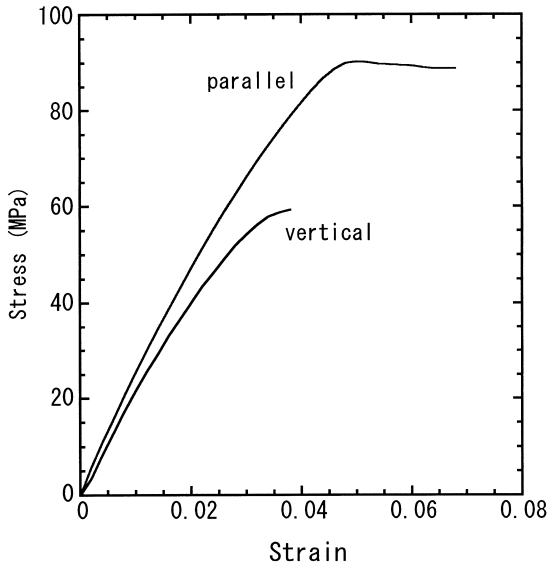

Fig. 14. Stress–strain curves of the drawn annealed film of iPS/PPO = 7/3 blend with draw ratio 5 tested in the parallel and perpendicular direction.

strength of isotropic iPS/PPO blends (58 MPa) is higher than that of iPS and PPO (45.6 and 55 MPa, respectively). The mechanical properties of atactic polystyrene (aPS) and PPO system were studied as a function of composition [18]. The fracture behavior is varied with composition of the a-PS/PPO blend from brittle behavior at low PPO content to ductile one at high PPO ratios. The analogous effects of blending PPO on the mechanical properties were expected for the iPS/PPO system. Blending PPO with iPS improved the brittleness of the oriented iPS in the perpendicular direction. The molecular orientation is also one of the important factors affecting the perpendicular strength. The orientation relaxation of amorphous chains of PPO and iPS improves the mechanical properties in the perpendicular direction by restricting the fibrillation of iPS.

Table 1
Mechanical properties of as-drawn films of iPS/PPO (before heat-treatment)

iPS/PPO	Draw ratio	Ultimate strength (MPa)		Dynamic storage modulus (GPa)	
		∥	⊥	∥	⊥
10/0	1	45.6		2.87	
	3	141.9	37.6	3.23	2.76
	5	182.6	27.3	3.25	2.27
7/3	1	58.0		2.72	
	3	74.9	53.2	2.67	2.69
	5	69.5	51.4	2.80	2.62
5/5	1	66.6		2.34	
	6	104.1	62.6	2.66	2.28
3/7	1	69.3		2.72	
0/10	1	55.0		2.26	

Table 2
Mechanical properties of drawn and heat-treated films of iPS/PPO

iPS/PPO	Draw ratio	Ultimate strength (MPa)		Dynamic storage modulus (GPa)	
		∥	⊥	∥	⊥
10/0	1	50.2		2.94	
	3	92.8	20.5	3.74	2.75
	5	109.5	13.8	4.67	2.28
7/3	1	68.4		2.64	
	3	78.7	61.3	2.89	2.43
	5	90.3	59.3	4.05	2.27
5/5	1	79.5		2.65	
	6	76.7	73.7	2.27	2.14

4. Conclusion

Oriented films of iPS/PPO blends were prepared by drawing the quenched blend films. The films were heat-treated under constraint at the drawing temperature so as to crystallize the molecular chains of iPS in the oriented state. The degree of crystallinity is much increased by heat-treating the oriented film of pure iPS and iPS/PPO = 7/3 blend. The polarized FTIR shows that the molecular chains of both iPS and PPO are oriented in the as-drawn sample (before annealing). In the FTIR spectra of annealed sample, however the large dichroism disappears for the absorption bands of PPO, and the absorption intensities of the 3_1 helix bands of iPS increase with the large dichroism retained. The orientation of amorphous molecular chains of iPS with disordered conformation is also relaxed by the heat-treatment. It was concluded that the drawn annealed samples of the iPS/PPO = 7/3 blend consist of highly oriented iPS crystals and nearly isotropic amorphous materials of PPO and iPS. The ultimate strength of the drawn annealed film of the iPS/PPO = 7/3 blend is improved in the drawing direction relative to the isotropic sample, and is a little lowered in the perpendicular direction. The ultimate strength in the perpendicular direction is 4–5 times higher in the drawn annealed film of iPS/PPO = 7/3 blend than in the drawn annealed pure iPS. The increase in the vertical strength in the iPS/PPO = 7/3 blend is considered to originate from the synergetic effect of the iPS/PPO blend and the orientation relaxation of the amorphous molecular chains of PPO.

Acknowledgements

The authors wish to thank Mr Yoshihisa Sugoh of A & D Co. Ltd, for the measurements of dynamic viscoelasticity, and are grateful to Dr Kazuo Nakayama of National Institute of Advanced Industrial Science and Technology for helpful advice on the measurement of dynamic viscoelasticity. A.K. Dikshit thanks Japan Society for the Promotion of Science

(JSPS) for the JSPS fellowship and for giving him a chance to study this work in National Institute of Advanced Industrial Science and Technology.

References

[1] Wenig W, Karasz FE, Macknight WJ. J Appl Phys 1975;46:4194.
[2] Hammel R, Macknight WJ, Karasz FE. J Appl Phys 1975;46:4199.
[3] Runt JP. Macromolecules 1981;14:420.
[4] Lefebvre D, Jasse B, Monnerie L. Polymer 1981;22:1616.
[5] Lefebvre D, Jasse B, Monnerie L. Polymer 1984;25:318.
[6] Bouton C, Arrondel V, Rey V, Sergot Ph, Manguin JL, Jasse B, Monnerie L. Polymer 1989;30:1414.
[7] Abtal E, Prud'homme RE. Macromolecules 1994;27:5780.
[8] Keroack D, Zhao Y, Prud'homme RE. Polymer 1998;40:243.
[9] Zhao Y, Keroack D, Prud'home R. Macromolecules 1999;32:1218.
[10] Kimura T, Ezure H, Tanaka S, Ito E. J Polym Sci, Part B: Polym Phys 1998;36:1227.
[11] Matsuba G, Kaji K, Nishida K, Kanaya T, Imai M. Polym J 1999;31: 722.
[12] Radhakrishnan J, Dikshit AK, Kaito A. J Polym Sci, Part B: Polym Phys 2000;38:2912.
[13] Kobayashi M, Tsumura K, Tadokoro H. J Polym Sci, Part A: Polym Chem 1968;6:1493.
[14] Kobayashi M, Akita K, Tadokoro H. Die Macromoleculare Chemie 1968;118:324.
[15] Painter PC, Koenig JL. J Polym Sci, Part B: Polym Phys 1977;15: 1885.
[16] Takeda M, Iimura K, Ochiai S. J Polym Sci B 1966;4:155.
[17] Wellinghoff ST, Koenig JL, Baer E. J Polym Sci: Polym Phys Ed 1977;15:1913.
[18] Creton C, Halary J-L, Monnerie L. Polymer 1998;40:199.